PHYSICAL REVIEW C VOLUME 22, NUMBER 5 NOVEMBER 1980

Double beta decay of ^{82}Se

M. K. Moe and D. D. Lowenthal*
Physics Department, University of California, Irvine, Irvine, California 92717
(Received 24 March 1980)

Pairs of negative beta particles have been observed originating from a ^{82}Se source during a cloud-chamber search for double beta decay. Backgrounds recognized in previous experiments were suppressed to well below the observed event rate, and no other significant backgrounds are apparent. Within the limited statistics of the small data sample, the observed single-electron energy spectrum, the two-electron sum energy spectrum, and the opening angle distribution are consistent with expectation for neutrino-accompanied double beta decay of ^{82}Se. The tentative assignment of the observed events to double beta decay, results in a ^{82}Se half-life of $(1.0\pm0.4)\times10^{19}$ years, in good agreement with some very recent theoretical predictions. However, the result is in serious disagreement with the much longer half-lives measured in geochemical experiments. A planned follow-up experiment is described.

[RADIOACTIVITY $\beta\beta$-decay ^{82}Se; measured $I_{\beta\beta}$; deduced $T_{1/2}$.]

I. INTRODUCTION

The theory of double beta decay and numerous experimental searches have been discussed extensively in the literature and summarized in a recent review article by Bryman and Picciotto.[1] The strong dependence of the theoretical half-life on the presence or absence of neutrinos accompanying double beta decay, has focused attention on the phenomenon as an extremely sensitive test of lepton conservation.

Although past experiments have not succeeded in directly observing double beta decay, either with or without neutrinos, indirect evidence from geochemical experiments[2-4] has indicated that double beta decay occurs. The geochemical evidence for ^{82}Se decay, together with a limit on neutrinoless decay from a direct counting experiment, has implied that decay with neutrinos is the predominant mode. The resulting upper limit[5] on the lepton number violating fraction of the weak interaction amplitude is $\alpha\sim3\times10^{-4}$. A geochemical measurement of the ratio of half-lives of two tellurium isotopes[4] has resulted in the still smaller limit $\alpha \leq 0.8\times10^{-4}$.

A recent comparison of experimental evidence with theory, however, has implied the occurrence of a small admixture of lepton-nonconserving neutrinoless decay,[1] but the suggestion of lepton number violation is not likely to be taken very seriously without evidence of a more direct kind.

The work reported here[6] is an attempt to extend the sensitivity of the direct counting technique by control of background. The offending backgrounds identified by Bardin *et al.*[7] in a ^{48}Ca experiment, consist of specific mechanisms by which ordinary beta emitters can cause two electrons to emerge together from the source. Implicated as the principal radioactive contaminant feeding these mechanisms was ^{214}Bi, a member of the naturally occurring uranium series.

The ^{214}Bi nucleus is short-lived. Its presence after a few days is maintained by its long-lived progenitor ^{226}Ra. The level of ^{226}Ra contamination that would prove troublesome is on the order of one part in 10^{15}. Although it may be possible by chemical purification techniques to achieve substantially lower levels of radium in isotopically enriched double beta sources,[8] success has not been adequately demonstrated. Alternatively, the approach used here is to make it much more difficult for contaminants, especially ^{214}Bi, to produce double-beta-like events.

Since ^{214}Bi beta decay is followed in 164 μs by emission of a 7.7 MeV alpha particle, bismuth-induced two-electron events can be identified if the alpha particle can be detected. The utility of a track visualizing device in double beta decay searches was demonstrated with a streamer chamber by Bardin *et al.*[7] If the 164 μs delayed alpha particle is to be seen, however, a sensitivity longer than that of a streamer chamber is required. A cloud chamber was chosen for the present experiment since the duration of post-trigger sensitivity easily embraces the delay of alpha particles attending bismuth decay.

A further requirement for detection of the alpha particle is that the double beta decay source be thin enough to ensure that the alpha particles are not trapped within. A trade-off between small source thickness and large source mass must be arranged if a realistic double beta event rate is to be expected in a chamber of reasonable size. For a source of finite thickness some alpha particles

TABLE I. Sources used in recent $\beta\beta$ experiments. (All background columns normalized to give unity for present experiment.)

Experiment	$\beta\beta$ isotope	Atoms of $\beta\beta$ isotope in source ($\times 10^{23}$)	Thickness of source (mg/cm^2)	Relative background per atom of $\beta\beta$ isotope [a] From Møller and Compton scattering From ^{214}Bi	From Møller and Compton scattering From contaminants without delayed alphas	From internal conversion From ^{214}Bi [b]	From internal conversion From contaminants without delayed alphas
Bardin *et al.* 1970	^{48}Ca	1.29	27	16	3.6	4.3	1.0
Cleveland *et al.* 1975	^{82}Se	1.91	58	34	7.8	4.3	1.0
Moe and Lowenthal 1979	^{82}Se	0.98	7.5	1.0	1.0	1.0	1.0

[a] Assuming equal radioactive contamination per atom of $\beta\beta$ isotope.
[b] Assuming 77% detection efficiency for ^{214}Bi alpha particles in present experiment.

emitted nearly in the plane of the source will never escape. Consequently, some fraction of the ^{214}Bi background will remain unidentified by the alpha technique. The source thickness was designed for an alpha escape probability of ~80%.

In addition to ^{214}Bi there may be other source contaminants lacking a delayed alpha particle yet able to produce negatron pairs. Scattering and internal conversion are the processes involved.

For a source in a cloud chamber with a magnetic field, the scattering of concern is of two kinds. A beta particle emitted within the source can drive out a second electron by Møller scattering. Alternatively, Compton scattering by a photon from a beta-gamma cascade within the source can supply the second electron.

With a given source mass, these processes occur in proportion to the source thickness. There are other less probable mechanisms that involve double scattering and occur as the source thickness squared. Since the source was designed to permit escape of ~80% of the ^{214}Bi alpha particles, it is much thinner than any used in previous double beta decay experiments. Hence a significant reduction should be seen in the scattering-associated background induced by *any* source contaminant (see Table I).

Internal conversion following beta decay is the other background mechanism to be considered. (Additional mechanisms for negatron pair production are known,[9] but these generally give rise to second electrons of very low energy.) For a given source mass, this process is independent of source thickness. It is difficult to build in discrimination against beta internal-conversion events for contaminants having no delayed alpha particle. One possibility is to strive for sufficient energy resolution to isolate the discrete energies of conversion electrons, although this technique was not fully implemented here. To the extent that ^{214}Bi is the cause of background from internal conversion, however, delayed alpha particle detection will bring about a significant reduction (Table I).

II. EXPERIMENTAL APPARATUS

A. The source

1. Isotope selection

^{82}Se was selected for the present experiment because of the favorable decay energy (3.0 MeV), chemical stability in the elemental form, relatively low atomic mass, availability in highly enriched form, and geochemical evidence for a half-life seemingly within range of a direct counting experiment.

2. Source fabrication

A 38 g sample of selenium, enriched to 97% ^{82}Se, was obtained on loan from Oak Ridge National Laboratory. This material had been inventoried in 1972 and had not been used for any previous experimentation.[8] The selenium was received as a gray metallic powder which had to be converted into a thin, uniform source compatible with the cloud-chamber environment.

The largest source area could be accommodated by an arrangement of parallel strips viewed edge-on (Fig. 1). For proper illumination of electron tracks among them, it was necessary that the strips have a highly reflective, specular surface. Each strip was constructed as a sandwich consist-

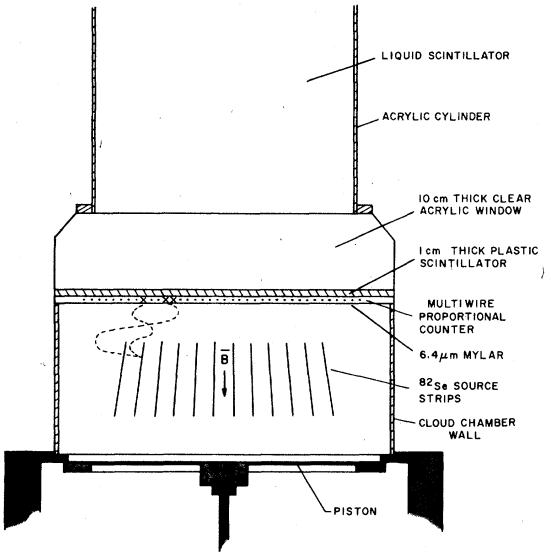

FIG. 1. Cross-sectional view of the cloud chamber, with a double beta decay event producing a two-electron signature in the multiwire proportional counter.

ing of two sheets of aluminized Mylar with selenium deposited uniformly on the inside surfaces.

It can be shown that for such a configuration the probability that an alpha particle originating in the selenium will escape to the outside is

$$P_\alpha = 1 - \frac{T}{2a} - \frac{t}{b},$$

where T equals the thickness of ^{82}Se, t equals the thickness of one Mylar sheet, a is the range of 7.7 MeV alpha particles in ^{82}Se, and b is the range in Mylar. With $b \cong a \cong 42$ μm, and $t = 3.8$ μm, the thickness (T) that will give an escape probability (P_α) of ~80% is ~9 μm or ~5 mg/cm^2.

This thin deposit of selenium was produced by evaporation in an atmosphere of argon from which the condensed particles settled by gravity onto a Mylar substrate.[10]

Microscopic examination of the source at this stage showed the deposit to be uniform down to a scale of ~$\frac{1}{5}$ of the alpha particle range. Two such selenium deposits were placed face-to-face and sealed together around the perimeter to form a single source strip. The strip thickness was 7.48 mg/cm^2, consisting of 5.60 mg/cm^2 of ^{82}Se, 1.08 mg/cm^2 Mylar, and ≤ 0.8 mg/cm^2 Formvar. The corresponding value of P_α is 0.77. A total of 13.75 g of selenium (of which 13.34 g were isotope 82) was included in 12 of these source strips of varying lengths. Losses of the precious enriched selenium were held to ~50 mg or 0.4%.

Care was taken at each step to avoid introducing additional contamination. All materials used were first checked in a low background gamma detection facility. The gamma spectra showed no evidence of uranium or thorium series radionuclides in the source materials. In the case of Formvar and its solvents it was possible to check samples more than an order of magnitude larger than were actually used. However, for the small samples of Mylar and ^{82}Se, the sensitivity of the NaI detector was insufficient by an order of magnitude to reveal radium at the <1 part in 10^{15} level required for a successful experiment. The actual contamination level had to await cloud chamber observation.

The source strips were suspended under tension between two brass rings and oriented to give edge-on appearance to the cameras. A clearing field was provided for ionization in the cloud chamber by a positive 15 V potential on every other strip, the remaining strips being grounded. Electrical conductivity was provided by the aluminized surface.

B. The cloud chamber, shielding, trigger scheme, and photography

The 46 cm diameter by 20 cm high cylindrical cloud chamber is illustrated in Fig. 1. The chamber and controls, built for a quark search,[11] were received as surplus upon completion of that experiment. The system was extensively modified for the present work, and located on the ground floor of the University of California–Irvine, Physical Sciences Building.

Although the sensitive time of the cloud chamber is long, typically 300 ms following expansion, the sensitivity is far too short to permit a reasonable accumulation of live time by random expansions. A trigger sensitive to pairs of electrons had to be developed. The 3 min recovery time of the chamber imposed the further condition that the trigger not respond to uninteresting activity more than once every few minutes, or excessive dead time would result.

The heart of the triggering scheme is a transparent multiwire proportional counter across the top of the chamber volume. The 36 wires operate as independent counters and provide spatial and temporal information necessary to discriminate against single electron events.

In Fig. 1 an imaginary double beta decay event is illustrated with the electron tracks emerging from a common point on one of the source strips. The electrons follow helical paths in the vertical magnetic field until they penetrate the 6.4 μm Mylar diaphragm that separates the argon-ethanol-water atmosphere of the cloud chamber from the argon-carbon-dioxide mixture in the 36-wire proportional counter. The side of the diaphragm facing the pro-

portional counter wires is coated with Inconel to provide electrical conductivity, while leaving the diaphragm transparent to visible light. Gas is flowed through the proportional counter continuously. Since the Mylar is incapable of sustaining a pressure differential, it moves freely during chamber expansions. A knife edge mounted centrally on the underside of the Mylar diaphragm cuts an infrared beam to control the counter gas flow in such a way as to maintain the normal diaphragm position to close tolerance. The cloud chamber and proportional counter operate at a gauge pressure of 0.34 bars.

Once inside the proportional counter, the electrons of Fig. 1 cause pulses on the wires in a manner recognized by the logic circuitry as a two-electron signature, namely, simultaneous pulses on two or more wires with one or more untriggered wires in between.

The electrons next enter and stop in a plastic scintillator which is used to impose a 1 MeV threshold on their sum energy. The lower side of the plastic scintillator is also coated with conductive, transparent Inconel. Scintillation light is transmitted upward through a 10-cm-thick acrylic window and an 84 cm column of liquid scintillator.

The photomultipliers that receive this light at the top of the column are shown in Fig. 2. Also shown, just above the photomultipliers, are the cameras that provide stereo photographs of the cloud chamber through the liquid scintillator, acrylic window, plastic scintillator, and proportional counter, all of which are transparent.

The liquid scintillator in the column serves to anticoincidence cosmic rays that pass through the column. (It also serves as a gamma-ray shield and light pipe for the plastic scintillator below.) Other cosmic rays are vetoed by a large area proportional counter anticoincidence detector just inside the iron shield.

The chamber is illuminated by xenon flash lamps, the light being collimated horizontally, and generally directed parallel to the source strips. The depth of the illuminated region is limited to 10 cm by the space between the magnet coils. Protection of the photomultipliers is arranged by driving the first dynode 20 V negative in anticipation of the flash. Peripherally displayed in the cloud chamber photographs are a LED hodoscope indicating which of the proportional counter wires

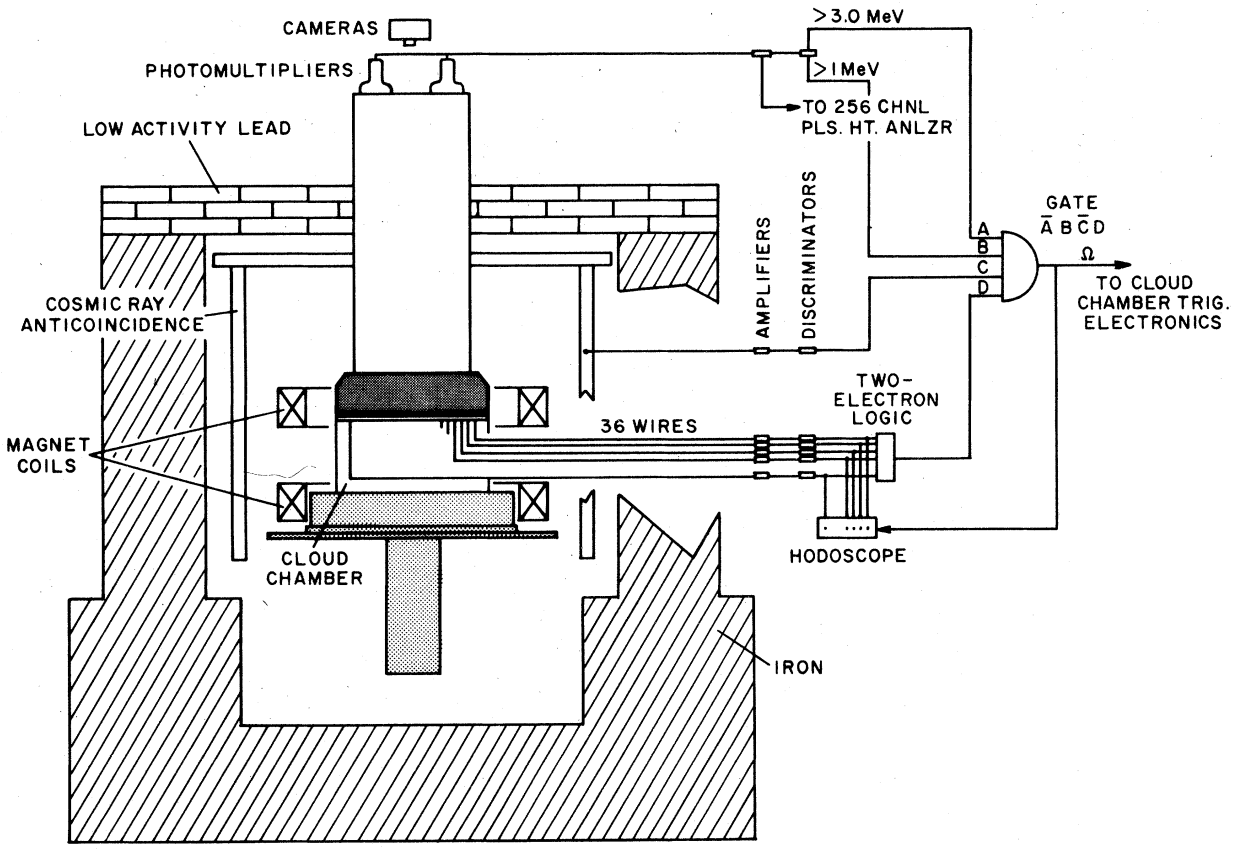

FIG. 2. Cutaway view of the cloud chamber in its shield.

TABLE II. The screening of unwanted activity by the various components of the trigger scheme.

	Counts per minute Single [a]	Two [b]
1. Multiwire proportional counter	2000	60
2. Multiwire proportional counter with a. gamma ray shield added	760	24
3. Multiwire proportional counter with a. gamma ray shield b. cosmic rays vetoed	63	15
4. Multiwire proportional counter with a. gamma ray shield b. cosmic rays vetoed c. 1 MeV energy threshold	11	0.33

[a] A "Single" event is a pulse above threshold from any wire or combination of wires in the multiwire counter.
[b] A "Two" event is any two-or-more-wire event with at least one blank wire somewhere in between.

participated in the trigger, a digital pulse height display corresponding to the scintillator pulse, a serial counter, and a clock.

The photographs subsequently are scanned through a stereoscopic viewer. Measurements of interesting events are made by moving cross hairs in the x and y directions with micrometer screws. A set of cross hairs and micrometers is provided for each of the two views. The micrometer readings are converted into the original three dimensional coordinates of the cloud chamber space with a precision of ±0.5 mm in the x and y direction, and ±3 mm in the z (vertical) direction.

The iron shield has a minimum wall thickness of 38 cm and forms a square well in which the cloud chamber rests. The top is closed with 15 cm of lead.

A valid cloud chamber trigger pulse is generated when the condition $\bar{A}\cdot B\cdot\bar{C}\cdot D$ is satisfied. Here $(B\cdot D)$ represents a two-electron trigger from the proportional counter and an energy pulse between 1.0 and 3.0 MeV from the photomultipliers. $(A\cdot C)$ represents a photomultiplier pulse >3.0 MeV or a pulse from the large area proportional counters. Table II indicates how the various parts of the apparatus contribute to reducing the trigger rate.

A magnetic field, measured with a calibrated Hall probe to be 1030 ± 30 G over the illuminated portion of the chamber, is provided by a near-Helmholtz configuration of magnet coils. The measurements were made with the iron shield in place.

Calibration of the scintillation system is done with a ^{207}Bi conversion electron source as a primary standard. The 0.98 MeV conversion electron gives a full width at half maximum of ±29% at any one source position, and a ±15% variation of peak pulse height with radial movement from center to edge. A secondary standard is provided by the cosmic ray peak from the liquid. Further details of the apparatus have been reported elsewhere.[12]

III. RESULTS AND DISCUSSION

A. Observed events

A crude preliminary Monte Carlo calculation estimated the trigger efficiency for double beta events as ~7%. (A later, more refined version of this calculation took account of experience with actual scanning criteria and predicted an efficiency of 2.5%, as discussed in Sec. III E.) The 7% efficiency, combined with the 13.34 g mass of ^{82}Se and the 2.8×10^{20} yr geochemical half-life,[2] led to an anticipated event rate of 17 per year.

At the end of 37 live days, 36 negatron pairs from the source strips had been observed. Of these, 20 were clean events ($2e^-$) and 16 were accompanied by alpha particles ($2e^- + \alpha$) (Figs. 3 and 4). Single electrons also occasionally triggered the chamber, presumably by scattering out of and back into the proportional counter. Of these, 72

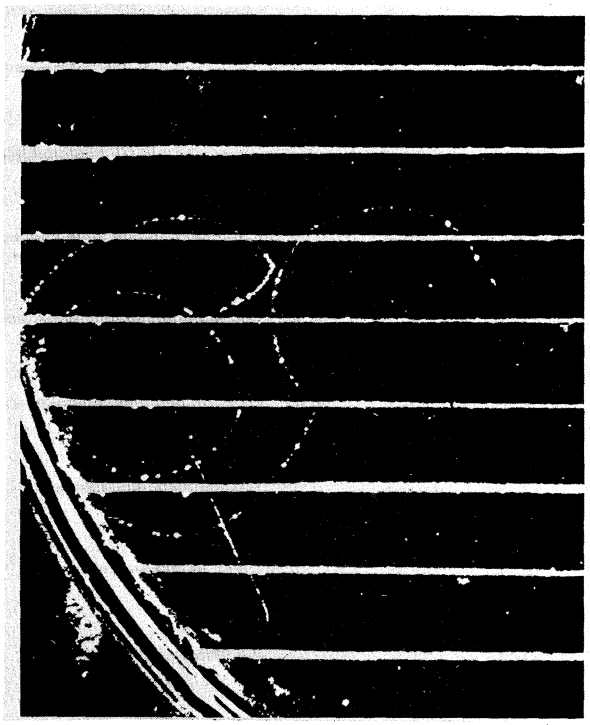

FIG. 3. A cloud chamber photograph of a negatron pair ($2e^-$) originating from one of the ^{82}Se source strips. The electrons pass through the strips quite freely.

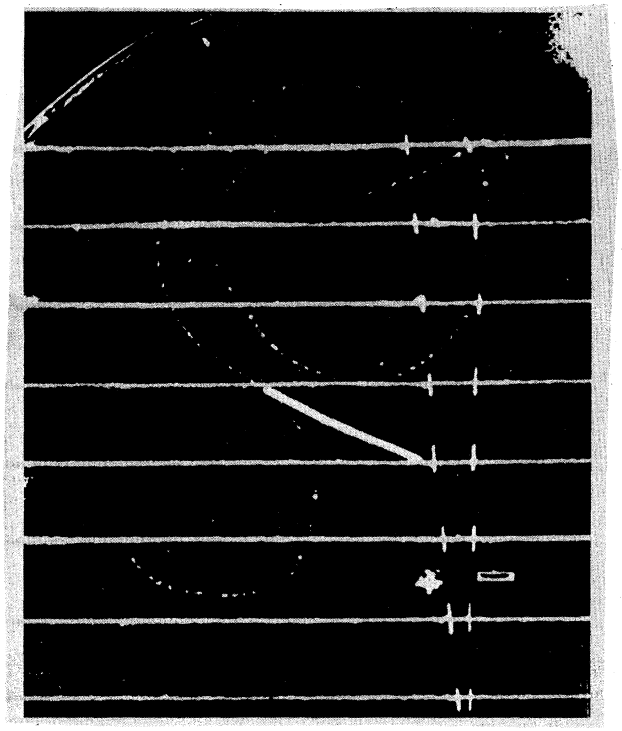

FIG. 4. A negatron pair from bismuth contamination as revealed by an accompanying alpha particle ($2e^- + \alpha$).

had an alpha particle ($e^- + \alpha$) at the origin on the ^{82}Se source. These three kinds of events are summarized in Table III.

B. Uranium and thorium series activity

1. Energetic beta emitters

Clearly the rate of negatron pair production was far in excess of the 17 events per year anticipated from double beta decay with the geochemical half-life, and the presence of alpha particles indicated that at least some of the negatron pairs arose from source contamination.

Table IV lists the naturally occurring beta emitters of the uranium and thorium series with decay energies >1 MeV.

2. ^{214}Bi

Two members of Table IV, ^{212}Bi and ^{214}Bi, have delayed alpha particles. The selenium source had been constructed to permit the escape of 77% of the alpha particles from ^{214}Bi. (The percentage of more energetic ^{212}Bi alpha particles escaping the source would be still greater.) The 77% escape probability can be written

$$\frac{N(2e^- + \alpha)}{N(2e^- + \alpha) + N(2e^-)} = 0.77,$$

where $N(2e^- + \alpha)$ is the number of $2e^- + \alpha$ events, and $N(2e^-)$ is the number of bismuth-induced $2e^-$ events where the unseen alpha particle is trapped within the source. Substituting the observed value 16 for $N(2e^- + \alpha)$ yields

$$N(2e^-) = 4.8 \pm 1.2$$

from ^{214}Bi. (Any admixture of ^{212}Bi would make this number smaller because of the greater alpha escape probability.) Since the observed number of $2e^-$ events was 20, it appeared that ^{214}Bi could be responsible for only about one-fourth of them.

3. Radon injections

Because the above limit on bismuth background required the use of a calculated 77% escape probability for alpha particles, a direct measurement of this probability was appropriate. Likewise, an understanding of the behavior of alpha-deficient beta emitters listed in Table IV was needed. A source doped with the suspected contaminants

TABLE III. Observed events and their ratios on negative and positive source strips.

	$e^- + \alpha$		$2e^- + \alpha$		$2e^-$		$\frac{N(2e^- + \alpha)}{N(e^- + \alpha)}$
	No. of events	$\frac{N(0\text{ V})}{N(+15\text{ V})}$	No. of events	$\frac{N(0\text{ V})}{N(+15\text{ V})}$	No. of events	$\frac{N(0\text{ V})}{N(+15\text{ V})}$	
Pre-injection (37.0 live days)	72	1.9 ± 0.5	16	1.7 ± 0.7	20	1.0 ± 0.4	0.22 ± 0.06
^{220}Rn injection Thorium series ^{212}Bi, ^{208}Tl	127	1.8 ± 0.3	2		17	1.4 ± 0.7	0.016 ± 0.011
^{222}Rn injection Uranium series ^{214}Bi	262	1.8 ± 0.2	48	1.2 ± 0.3	15	2.8 ± 1.6	0.18 ± 0.03

TABLE IV. Potential radioactive contaminants from the uranium and thorium series.

Radioactive contaminant	Q_{β^-} Total energy available to beta-gamma cascade (MeV)	Prompt alpha particle[a] Energy (MeV)	Prompt alpha particle[a] Delay (μs)	Contribution to the 20 observed $2e^-$ events	
Uranium series					
$^{234}Pa^m$	2.29			$\lesssim 1$	Limited by rate of single electrons (Sec. III B 7 *c*). Also inconsistent with observed spectrum.
^{214}Pb	1.03			~ 0	Insufficient energy (Sec. III B 6)
^{214}Bi	3.26	7.68	164	4.8 ± 1.2	Alphas trapped in source (Sec. III B 2)
^{210}Bi	1.16			~ 0	Insufficient energy (Sec. III B 6)
Thorium series					
^{208}Tl	4.99			$\lesssim 1$	Lack of ^{220}Rn (Sec. III B 5)
^{228}Ac	2.14			$\lesssim 1$	If series in equilibrium (Sec. III B 7 *c*). Also inconsistent with observed spectrum
^{212}Bi	2.25	8.95	0.30	$\ll 1$	Lack of ^{220}Rn (Sec. III B 5)

[a] An alpha decay following a beta decay within a tenth of a second is defined as "prompt."

would provide an informative test.

The fabrication and doping of new source strips was an unpleasant prospect involving the possibility of contaminating the laboratory with the very materials most dreaded. A peculiar asymmetry in the distribution of alpha-accompanied events among the 12 source strips gave a clue as to how temporary doping of the existing source might be accomplished simply and without risk.

The source strips that were held at ground potential were the site of nearly twice the $e^- + \alpha$ and $2e^- + \alpha$ events as the strips held at positive 15 V (Table III). Apparently contaminants of predominantly positive charge were being attracted to the "negative" (grounded) strips. The migration of alpha activity is well known and occurs through the mobility of radon gas. When radon decays the daughters have a probability of approximately $\frac{2}{3}$ for carrying a net positive charge and $\frac{1}{3}$ for negative charge.[13] The approximate 2 to 1 ratio of alpha particles from negative source strips to those from positive strips implicated radon as the carrier of the observed alpha activity.

If excess ^{222}Rn from the uranium series were to be injected into the cloud chamber, an equilibrium distribution of daughters down to ^{210}Pb would be established in a few hours. These daughter nuclei, including ^{214}Bi, would adhere to the source surfaces according to the 2 to 1 ratio described above. The resulting activity would diminish with the 3.8 d half-life of the radon. Only 22-yr ^{210}Pb and its progeny would persist beyond a few weeks, and their activity would be down from the injected radon activity by the 5×10^{-4} ratio of the ^{222}Rn and ^{210}Pb half-lives.

The only member of Table IV in this low level residue is ^{210}Bi, which, as will be shown, has insufficient decay energy to contribute significantly to the observed energy spectrum. Hence an injection of ^{222}Rn into the cloud chamber would safely dope the source with the interesting uranium series members of Table IV, with the exception of $^{234}Pa^m$.

Similarly an injection of ^{220}Rn would safely dope the source with all thorium series members of Table IV except ^{228}Ac. Here the decay of the interesting daughters is controlled by ^{212}Pb with an 11 h half-life.

Because of the shorter decay time of the ensuing series, ^{220}Rn was injected first. The gas was passed through a filter to remove any accompanying long-lived parent. The short half-life (54 sec) of ^{220}Rn required that it be flushed quickly into the cloud chamber and mixed by a series of expansions. Data on ^{212}Bi and ^{208}Tl were collected until the trigger rate was down to 4 times the pre-injection rate. The results appear in Table III.

After the thorium series activity had died away, a similar injection procedure was carried out with ^{222}Rn of the uranium series. These data also appear in Table III.

4. Measurement of probability of alpha particle escaping the source

The radon injections gave a direct measurement of the probability $P_\alpha(^{214}\mathrm{Bi})$ that alpha particles will escape the source and be seen following ^{214}Bi decay. (It can be shown that this probability is independent of the location of the bismuth on or within a source if the total source thickness is less than the alpha particle range.)

$$P_\alpha(^{214}\mathrm{Bi}) = \frac{N(2e^- + \alpha)}{N(2e^- + \alpha) + N(2e^-)}$$

$$= \frac{48}{48 + 15} = 0.76 \pm 0.05 ,$$

which agrees well with the 0.77 value calculated from the source thickness and alpha particle range, and supports the earlier conclusion that bismuth is responsible for only a small fraction of the 20 pre-injection $2e^-$ events. (Note that the ratio $N(0\ \mathrm{V})/N(+15\ \mathrm{V})$ for pre-injection $2e^-$ events in Table III does not show the characteristic 1.8 value of radon daughters.)

5. ^{208}Tl and ^{212}Bi

A second implication of the gas injection results is that thorium series activity descending from ^{220}Rn is not present in sufficient quantity to account for the pre-injection $2e^-$ events. The paucity of $2e^- + \alpha$ events following the ^{220}Rn injection shows that ^{212}Bi, with its 2.25 MeV beta decay, is inefficient at producing electrons in pairs. The seventeen $2e^-$ events associated with ^{220}Rn had to come from ^{208}Tl.

The ratio $N(2e^- + \alpha)/N(e^- + \alpha)$ produced by ^{220}Rn is in gross disagreement with the pre-injection results (last column of Table III), while the ratio produced by ^{222}Rn agrees with the pre-injection ratio quite well. It follows that there could be relatively little ^{220}Rn contributing to the pre-injection activity. A limit of one event from ^{208}Tl can be calculated, and the contribution from ^{212}Bi can be shown to be completely negligible.[10]

6. ^{210}Bi and ^{214}Pb

Table IV contains two more nuclides that are easily eliminated by their low decay energies, namely ^{214}Pb at 1.03 MeV, and ^{210}Bi at 1.16 MeV. Such energies are insufficient to produce the measured spectrum shown in Fig. 12.

7. ^{228}Ac and ^{234}Pa^m

a. Limit on activity present. The only worrisome contaminants in Table IV which have not been addressed are ^{228}Ac and ^{234}Pa^m. Because these nuclides precede rather than follow radon in their respective decay series, they did not enter the cloud chamber with the radon injections. However, the rate at which these nuclides produce negatron pairs can be calculated if one knows their beta activity in the source, and the probability per beta decay of producing a negatron pair.

First, an attempt was made to place a limit on the amount of ^{234}Pa^m beta activity that could be present. The ~2 to 1 ratio of pre-injection alpha events on negative and positive source strips implied that the radon responsible was mostly in the cloud chamber gas and not confined within the selenium. The chamber typically remained sealed for many weeks, so the level of radon was being maintained by continuous decay of radium within the chamber.

The selenium envelope was shown to be impermeable to radon on the time scale of the radon half-life, and therefore the parent radium was somewhere outside of the selenium source. The selenium itself contained relatively little radium activity in comparison with activity from bismuth that settled on the outside surface of the Mylar.

The relative absence of radium activity in the source means that ^{234}Pa^m activity is absent there as well, if the decay series above radon is in equilibrium. Series equilibrium is not guaranteed, however, because of the long intervening half-lives of ^{230}Th and ^{234}U. It can be concluded that the ^{234}Pa^m beta activity in the source is limited to less than the ^{214}Bi beta activity if series equilibrium is assumed.

A similar line of reasoning can be used to tie the ^{228}Ac activity to that of lower members of the thorium series, this time with no doubts about series equilibrium, because the greatest intervening half-life (1.9 yr) is less than the time between sealing of the source and termination of the experiment.

An additional weakness in these series equilibrium arguments arises from the chance that ^{228}Ac or ^{234}Pa^m resides only on the *outer* surface of the source envelope where resulting radon could drift away without betraying its origin. This circumstance is considered unlikely, but nevertheless, should be recognized.

Another approach to a limit on beta activity from ^{228}Ac and ^{234}Pa^m, or any other contaminant, is to exploit a flaw in the cloud chamber triggering scheme, namely its occasional response to single beta particles. A count of triggers by single electrons that originate on the source strips would give an indication of the beta activity present.

Such a count was attempted, and the number of single beta particles from the source (with no accompanying α particle) was estimated as 180 ± 65 for the 37 live-day pre-injection period. A small

TABLE V. Limits on beta decay rates for ^{228}Ac and ^{234}Pa^m in the source.

Contaminant	A Observed single electron triggers (threshold 1 MeV)	B Fraction of β spectrum >1 MeV	Number of β decays occurring relative to decays of ^{214}Bi $\frac{A/B}{(A/B)_{^{214}Bi}}$
^{214}Bi	94	0.14	1
^{228}Ac	<84	0.05	<2.5
^{234}Pa^m	<84	0.35	<0.35

number of these can be attributed to beta decay of ^{214}Bi where the alpha particle is trapped in the source. The number of such trapped-alpha events is $[N(e^- + \alpha)][1 - P_\alpha]/P_\alpha$, where $N(e^- + \alpha) = 72$ and $P_\alpha = 0.77$. The resulting 22 ± 3 events can be subtracted from those above to give

$$(180 \pm 65) - (22 \pm 3) = 158 \pm 65 .$$

The single beta particle count can be further reduced by removal of the Compton scattering contribution. A measurement of the ambient gamma ray flux in the center of the shielded cloud chamber was used to calculate[10] the number of triggering single electrons from Compton scattering of ambient gamma rays as 168 ± 68.

If the Compton electrons are subtracted from the single beta particle count, there remain

$$(158 \pm 65) - (168 \pm 68) = -10 \pm 94$$

single electrons. The upper limit of 84 can be considered as a bound on the number of triggers by single electrons from beta decay of source contaminants other than ^{214}Bi. This limit is approximately equal to the known contribution from ^{214}Bi itself, namely, $N(e^- + \alpha)P_\alpha = 72/0.77 = 94$.

Any attempt to use this result to limit background must be done with an understanding of the decay scheme of the suspected contaminant. For example, if the beta decay is predominantly to a highly excited level of the daughter nucleus, the single beta particle energy may be too low to trigger the chamber, even though Q_β (the total energy available to the β-γ cascade) may be well above threshold. Contaminants such as ^{60}Co ($Q_\beta = 2.8$ MeV), with essentially none of the single beta spectrum above 1 MeV, could hide completely from the single electron count by this device.

By comparison, the fraction of the ^{214}Bi beta spectrum above 1 MeV is ~14%. For ^{228}Ac and ^{234}Pa^m the corresponding fractions are approximately 5% and 35%. These percentages can be combined with the limit of 84 single beta particles from the source to yield upper limits on beta decay of ^{228}Ac and ^{234}Pa^m relative to ^{214}Bi, as shown in Table V.

These beta decay limits will be used to restrict the actual $2e^-$ background from ^{228}Ac and ^{234}Pa^m. Attention is now directed toward the method of production of negatron pairs by these contaminants.

b. Internal conversion as the predominant background mechanism. Large variations in negatron pair production efficiency occur among the radionuclides, as was seen dramatically in the case of ^{212}Bi and ^{214}Bi. The relative lack of two-electron events from ^{212}Bi cannot be assumed to result from its lower decay energy, because single electrons from this isotope $(e^- + \alpha)$ triggered the chamber quite readily. Since ^{212}Bi beta decays predominantly to the ground state, and ^{214}Bi goes mostly to excited levels, the relative absence of $2e^- + \alpha$ events from ^{212}Bi suggests that ground state transitions are ineffective at negatron pair production. Ground-state decays can produce pairs via the Møller mechanism, which apparently is contributing insignificantly. Since the appropriate Møller scattering cross section is larger than the corresponding Compton cross section, inefficiency of the Compton mechanism is also implied. Internal conversion emerges as the probable mechanism for production of background negatron pairs.

The predominance of internal conversion is supported by another feature of the data. Since the source strips are closely spaced, any scattering that produces a second electron by the Møller and Compton mechanisms has a comparable probability of occurring instead in a neighboring strip, as shown in Fig. 5. Events depicted in Fig. 5 were rarely observed. Scattering in these thin source strips is not a significant source of negatron pairs.

Having identified internal conversion as the predominant background mechanism, one can now calculate the negatron pair efficiency of ^{228}Ac and ^{234}Pa^m, and the energy spectra of the pairs produced.

c. Calculated energy spectra of beta internal-conversion pairs. The rather complex decay

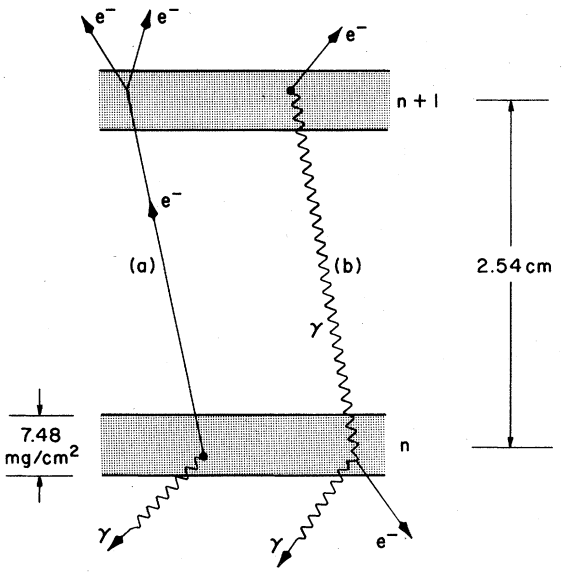

FIG. 5. (a) A beta particle from contamination in source strip n Møller scatters in strip $n+1$. The source thickness is shown exaggerated. View is from above, as in Figs. 3 and 4. (b) A photon from a beta-gamma cascade in a contaminant in source strip $n+1$ Compton scatters in strip n.

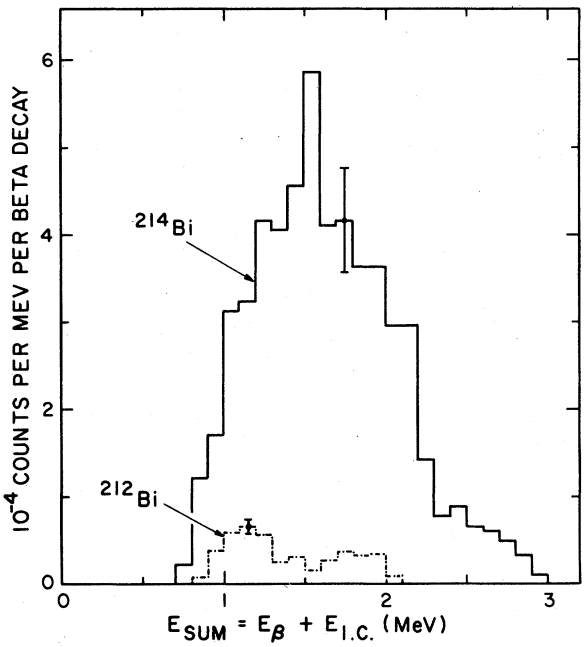

FIG. 6. Monte Carlo simulation of the sum energy spectra of beta internal-conversion pairs produced by ^{212}Bi and ^{214}Bi, as seen by the apparatus. Spectra are normalized per decay of the designated nuclide.

scheme[14] of ^{228}Ac was programmed into a Monte Carlo calculation for the purpose of generating a large set of beta internal-conversion pairs characteristic of this nucleus.

The program was run until the energies of the two electrons in each of 4000 beta internal-conversion pairs had been written into a data file. The production efficiency was calculated from the number of beta decays required to make the 4000 pairs, and the energy spectra of the pairs, both single and sum, were printed out in 0.1 MeV bins. As a check on the program, the resulting continuous beta spectrum and the absolute intensities of the conversion lines were noted to agree reasonably well with published data at energies above the 0.2 MeV single particle threshold.

A similar program was run for ^{214}Bi, ^{212}Bi, and ^{208}Tl. No program was run for ^{234}Pa^{m} because, as will be shown later, its decay scheme allows one to anticipate the results by inspection.

A second Monte Carlo program (cf. Sec. III E) took each of the 4000 pairs generated by the first program, placed its origin at a random position in the selenium source, and asked whether it would trigger the cloud chamber and result in an accepted $2e^-$ event. In this way, the output of the second program simulated the energy spectra one would measure if the corresponding contaminant were in the selenium source.

The results can be seen in Figs. 6 and 7, which display absolute intensities as would be seen by the cloud chamber, The areas under the histograms indicate the number of triggering negatron pairs per beta decay of the contaminant. As previously noted, ^{212}Bi is relatively innocuous.

The simulated ^{228}Ac sum spectrum is normalized and superimposed on the measured $2e^-$ spectrum

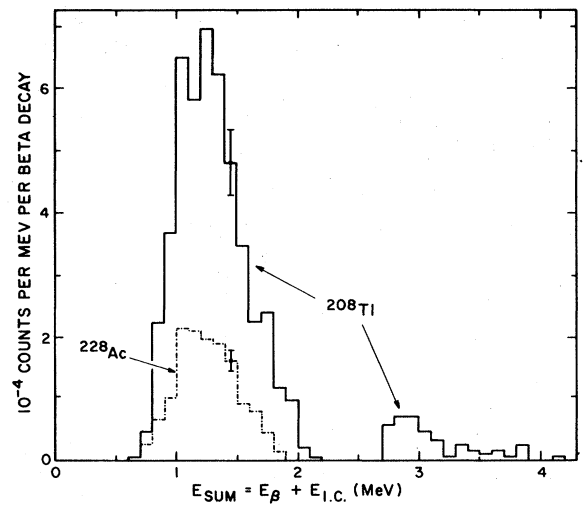

FIG. 7. Monte Carlo simulation of the sum energy spectra of beta internal-conversion pairs produced by ^{228}Ac and ^{208}Tl, as seen by the apparatus. Spectra are normalized per decay of the designated nuclide.

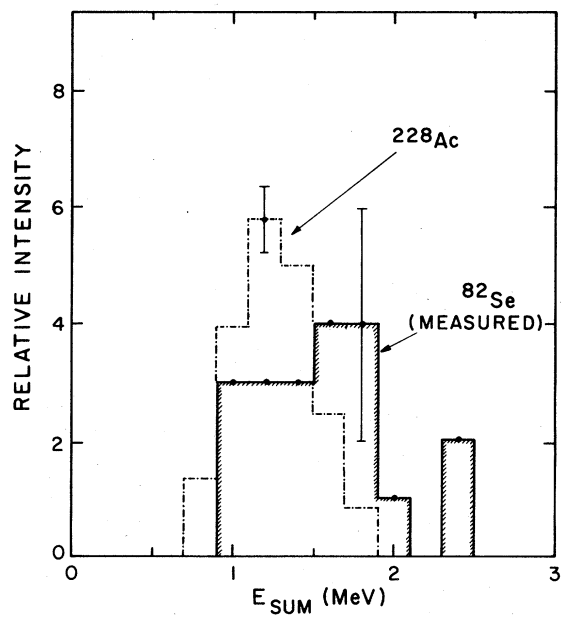

FIG. 8. Monte Carlo simulation of the sum energy spectrum of beta internal-conversion pairs produced by ^{228}Ac, and the measured sum spectrum of the twenty $2e^-$ events from the ^{82}Se source.

in Fig. 8. The ^{228}Ac energies are lower than those of the measured events, the respective mean energies being 1.25 and 1.54 MeV. The corresponding spectra of 40 *single* electrons belonging to these negatron pairs show a similar disparity.[10]

It will be recalled that the measured spectrum contains approximately 25% ^{214}Bi. As will be shown in later sections the ^{214}Bi and measured ^{82}Se spectra are quite similar. Therefore, subtraction of a 25% ^{214}Bi component would not significantly alter the shape of the measured spectrum.

The potency of ^{228}Ac in Fig. 7 is only 27% that of ^{208}Tl. If the thorium series is in equilibrium as expected between ^{228}Ac and ^{208}Tl, then, because of the branching ratio at ^{212}Bi, ^{228}Ac would be contributing 81% as many negatron pairs as ^{208}Tl. Since ^{208}Tl was shown to be limited to ~1 background event, the ^{228}Ac contribution would likewise be insignificant (Table IV).

It can also be shown that ^{234}Pa^m is inconsistent with the results measured for $2e^-$ events produced by the selenium source. Beta decays of ^{234}Pa^m go directly to the ground state with a probability of 98.6%. Only the remaining 1.4% can include internal conversion. A line at 0.696 MeV, absolute intensity 0.40%, is the only significant K conversion above threshold. (The L line at 0.790 MeV has intensity 0.078%.[15]) The spectrum of single electrons associated with beta internal-conversion pairs from ^{234}Pa^m would be strongly dominated by the 0.696 MeV K line. There is no evidence for this domination in the measured single electron spectrum of Fig. 12.

A quantitative limit on pairs from ^{234}Pa^m can be derived as follows. The 0.696 MeV conversion electron requires an additional 0.304 MeV from the beta particle to carry the pair over the 1 MeV sum threshold. The 1.48 MeV beta transition in coincidence with the conversion line gives a beta particle of sufficient energy ~65% of the time, for an overall negatron pair production efficiency of 0.65 $\times$0.40% = 0.26%. The corresponding efficiency for ^{214}Bi is 1.22% (from the decay scheme Monte Carlo calculation). The maximum number of pairs possible from ^{234}Pa^m, $P_{\max}(^{234}\mathrm{Pa}^m)$, therefore, can be scaled from the number of ^{214}Bi pairs as follows: the limit on pairs from ^{234}Pa^m equals the total observed pairs from ^{214}Bi multiplied by the ratio of negatron pair production efficiencies multiplied by the ratio of beta activities (Table V), i.e.,

$$P_{\max}(^{234}\mathrm{Pa}^m) = \frac{N(2e^- + \alpha)}{P_\alpha} \times \frac{\epsilon(^{234}\mathrm{Pa}^m)}{\epsilon(^{214}\mathrm{Bi})} \times \frac{N_\beta(^{234}\mathrm{Pa}^m)}{N_\beta(^{214}\mathrm{Bi})}$$

$$= \frac{16}{0.77} \times \frac{0.26}{1.22} \times 0.35 = 1.5 .$$

The corresponding calculation for ^{228}Ac yields 26 events. More stringent limits on this background have been found by other methods.

In view of these considerations, ^{214}Bi seems to be the only naturally occurring energetic beta emitter of Table IV capable of producing a significant background of negatron pairs, and the ^{214}Bi pairs without visible alpha particles account for only ~$\frac{1}{4}$ of the $2e^-$ events recorded.

C. Other possible contaminants

Additional radionuclides that might be suspected of contaminating the apparatus have been considered as possible sources of the $2e^-$ signal. These include the naturally occurring actinium series, the nonseries nuclides such as ^{40}K that occur naturally because of their long half-lives, nuclides produced continuously by cosmic rays, fallout from atmospheric testing of nuclear weapons, nuclides such as ^{83}Se that might be produced by neutron activation in the source, and man-made materials such as ^{60}Co.

All failed to meet one or more criteria for background production. These include a Q_β- of at least 2 MeV (a conservative value inasmuch as it required 3.2 MeV in the case of ^{214}Bi to mimic the measured spectrum of Fig. 8); large enough internal conversion coefficients to produce the observed negatron pairs and still be undetected in the initial gamma ray spectrum or the single electron count; a half-life greater than ~30 d or a

credible means of continuous production; and no prompt alpha particle.

A detailed account of these considerations can be found in Ref. 10. The contminants discussed are the more common and highly suspected ones. Any others that might be present could be troublesome only if they satisfy the criteria that eliminated those contaminants already considered.

D. Møller scattering of unseen incoming electrons

A conceivable background production mechanism, peculiar to the geometry of this experiment, involves the Møller scattering of electrons moving into the source array from below. [These electrons should not be confused with the ones coming from the source itself as depicted in Fig. 5(a).] Because the flash illumination extended only about one centimeter below the source strips, there was a possibility that some upward-coming electrons would lie closely in the plane of a source strip during their upward passage through the illuminated region, and thus not be seen in the photographs. Should such an unseen electron Møller scatter in the source, it would give the appearance of a spontaneous negatron pair.

The opening angle for Møller events is always less than 90° and is a function of the electron energies. A scatter plot of the twenty $2e^-$ events is shown in Fig. 9, where the ordinate is the measured opening angle, and the abscissa is the calculated Møller angle. There is no apparent clustering of measured angles about the Møller values.

A further check of the Møller possibility was carried out with a beta source placed on the bottom of the chamber. The pure beta spectrum of the ^{32}P source (end-point energy 1.71 MeV) was sufficiently intense to overwhelm other activity. The chamber was triggered in the usual manner with a 1.0 MeV threshold, and operated until 93 Møller scattering events had been observed, 45 in the gas and 48 in the source strips. Of these, only one had no visible "tail," that is, had the appearance of a "V" rather than a "Y." This event was at the bottom of a source strip where $2e^-$ events were normally rejected as being below the fiducial boundary. In the pre-injection data set the ratio of V's to Y's with the vertex on the source was approximately ten times greater than the 1 in 48 seen here. It was concluded that the $2e^-$ events arose from a cause other than Møller scattering of unseen incoming electrons.

E. The Monte Carlo calculation

The triggering scheme does not respond with equal efficiency for all electron pairs spawned by the selenium source. Biases in the energy spectra and opening angle distributions result from such features as the requirement that both electrons be directed upward toward the trigger counter, and the requirement for sufficient track curvature to establish the sign of the charge.

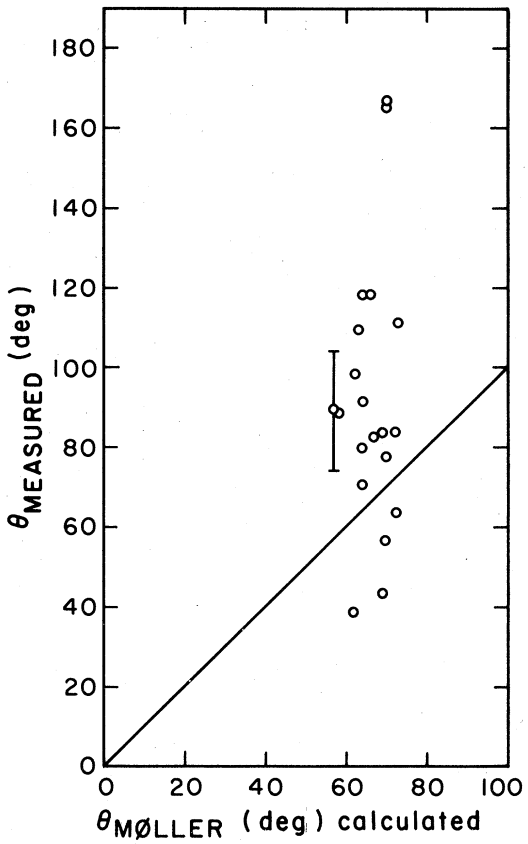

FIG. 9. Measured opening angle and Møller opening angle calculated from energies for each of twenty $2e^-$ events from the ^{82}Se source. There is no apparent clustering about the sloping line where the angles are equal.

To better understand the extent of these biases, and to estimate the detection efficiency of the apparatus, a Monte Carlo program was devised to simulate large numbers of actual events. Details of the calculation and the resulting energy spectra and opening angle distributions for ^{82}Se are reported in Ref. 10. A comparison of Monte Carlo and measured ^{214}Bi spectra appears in Figs. 10 and 11.

F. Goodness of fit of $2e^-$ data to ^{82}Se double beta decay

1. The energy spectra

Electron energies are measured from track curvature in the 1 kG magnetic field. The precision is best for tracks at right angles to the magnetic field and degrades with a decreasing angle. The best

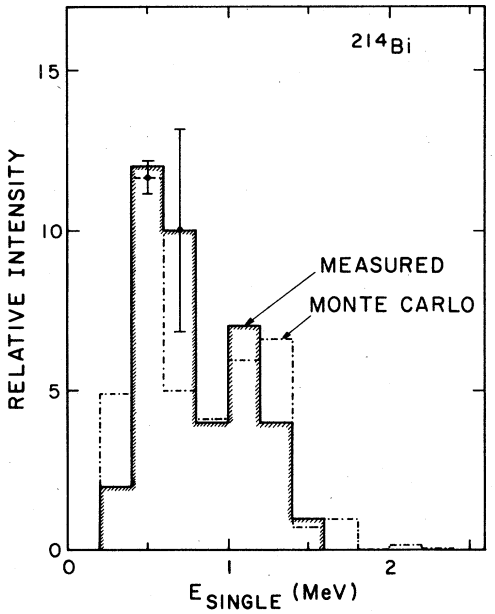

FIG. 10. The measured single electron energy spectrum of beta internal-conversion pairs from ^{214}Bi (twenty $2e^- + \alpha$ events). Superimposed is the normalized Monte Carlo ^{214}Bi spectrum in the apparatus.

energy measurements are good to ~±2% and the average resolution is judged, on the basis of reproducibility from different segments of the same track, to be within ~±15%.

The predicted ^{82}Se double beta decay, single electron energy spectrum is shown normalized to the measured spectrum of $2e^-$ events from the ^{82}Se source in Fig. 12. The probability of a larger χ^2 is 95%, i.e., the measured and predicted spectra are statistically consistent.

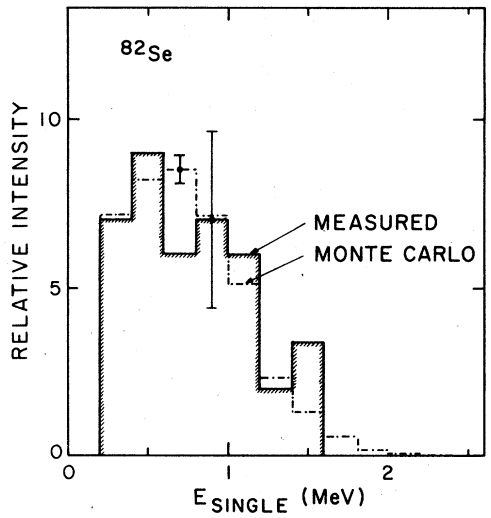

FIG. 12. The predicted and measured single electron energy spectra for negatron pairs from ^{82}Se.

The corresponding sum spectra appear in Fig. 13. As in the case of the ^{228}Ac comparison, the counts are somewhat fewer than desired for a χ^2 test, but if χ^2 is calculated, the probability of a larger value is 80%, again indicating that the measured and predicted histograms are statistically consistent. The predicted and measured mean sum energies are 1.50 and 1.54 MeV, respectively.

An alternative format for presentation of the energy data is the scatter plot, as shown in Figs. 14 and 15 for ^{82}Se and ^{214}Bi, respectively. In each case the dots represent 200 events generated by the Monte Carlo program. The two Monte Carlo distri-

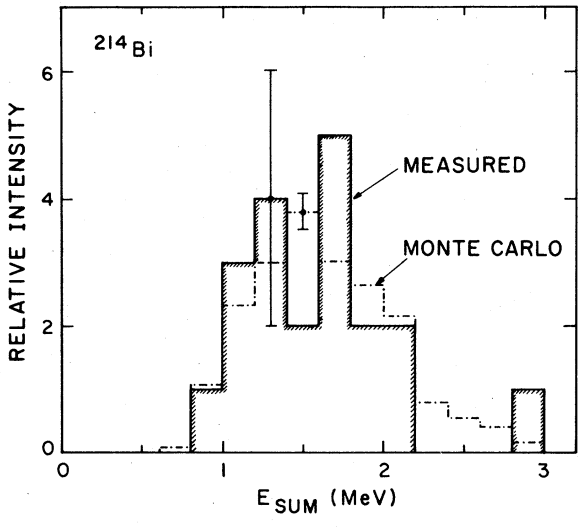

FIG. 11. The measured sum energy spectrum of beta internal-conversion pairs from ^{214}Bi (twenty $2e^- + \alpha$ events). Superimposed is the normalized Monte Carlo ^{214}Bi spectrum in the apparatus.

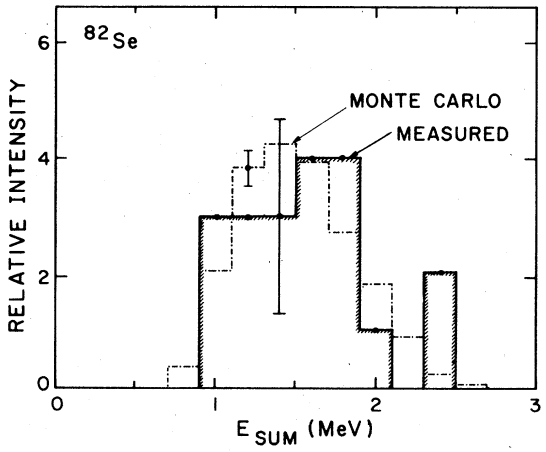

FIG. 13. The predicted and measured electron sum energy spectra for negatron pairs from ^{82}Se.

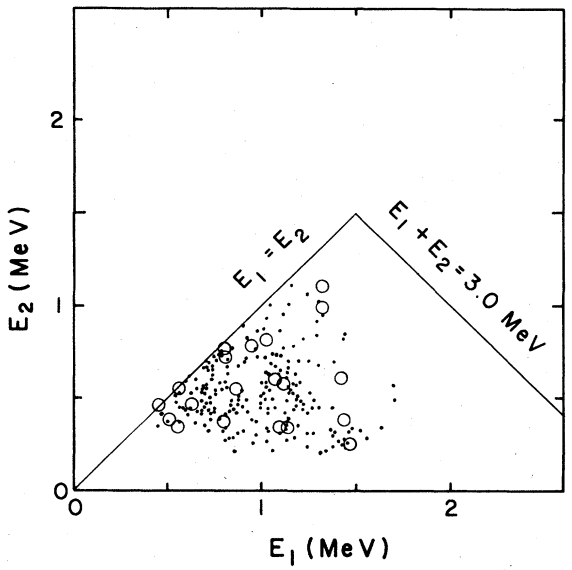

FIG. 14. Kinetic energies of 200 Monte Carlo generated pairs from ^{82}Se double beta decay (dots), and the measured $2e^-$ events (circles). E_1 is always taken to be the larger energy.

butions are quite distinctive, with the ^{214}Bi events clustering along the conversion lines. The measured data are shown as circles. Energy resolution smears the data somewhat, but the circles are generally consistent with their predicted distributions. (Roughly $\frac{1}{4}$ of the ^{82}Se events are known to be ^{214}Bi events with unseen alpha particles. See Sec. III B.)

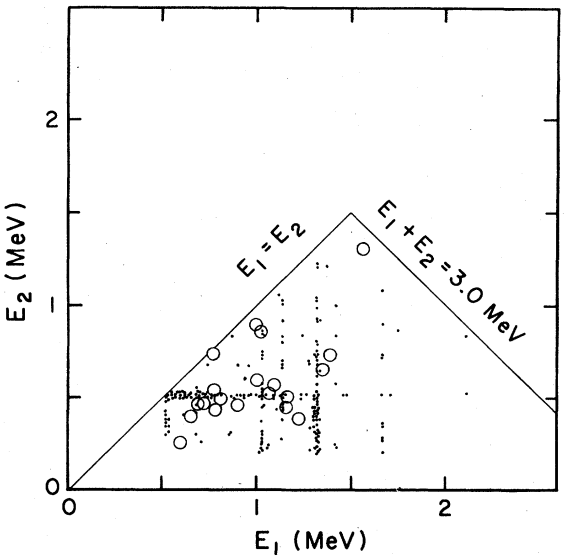

FIG. 15. Kinetic energies of 200 Monte Carlo generated pairs from ^{214}Bi beta decay with internal conversion (dots), and the measured $2e^- + \alpha$ events (circles). Again, E_1 is the larger energy.

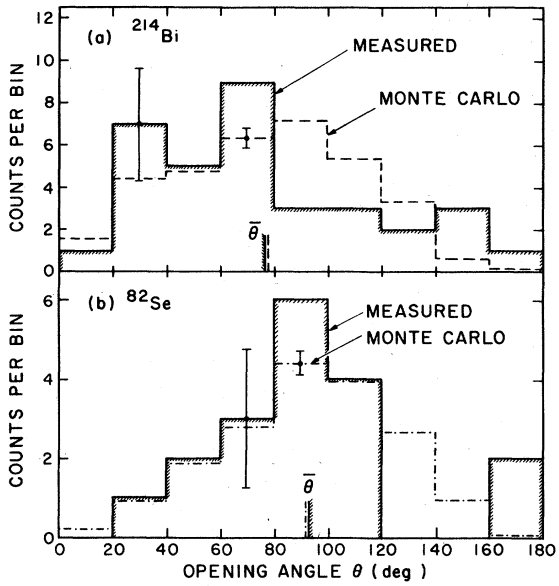

FIG. 16. Opening angle distributions (a) for beta internal-conversion pairs, using as an example ^{214}Bi as measured from thirty-four $2e^- + \alpha$ events, and as predicted by Monte Carlo for the apparatus, and (b) for 18 measured $2e^-$ events, and as predicted by Monte Carlo for ^{82}Se double beta decay in the apparatus.

2. *The opening angle distribution*

Opening angles can be measured with an accuracy estimated to be ±15°. The ^{82}Se double beta decay version of the Monte Carlo program, and the version for beta internal-conversion pairs from contaminants, predict rather different opening angle distributions for the two phenomena. The tendency of double beta decay to produce larger opening angles[10] survives the bias of the apparatus.

The shape of the distribution for beta internal-conversion pairs is weakly dependent on the particular contaminant being modeled. For ^{214}Bi the shape is reproduced as the broken line in Fig. 16(a), normalized to the distribution of 34 opening angles measured from initially upward directed ^{214}Bi pairs ($2e^- + \alpha$).

A comparison of measured and predicted opening angles is made for $2e^-$ events from the ^{82}Se source in Fig. 16(b). The measured sample is reduced from 20 to 18 events because those with initial downward velocity components were not included.

The mean opening angles of the four distributions are indicated in Fig. 16 and tabulated in Table VI. The assigned uncertainties include the measurement errors and the statistical uncertainty of the mean. The measured mean opening angle for the $2e^-$ events agrees with the ^{82}Se double beta decay prediction, and differs by two standard deviations from the contaminant value. The measured ^{214}Bi

TABLE VI. Mean opening angles (degrees).

	Predicted	Measured
^{82}Se double beta decay	92.4	($2e^-$ events) 92.7 ± 7.5
Contamination-caused beta internal-conversion pairs (^{214}Bi)	77.7	($2e^- + \alpha$ events) 76.7 ± 6.1

mean agrees with the contaminant prediction and differs by $2\frac{1}{2}$ standard deviations from the ^{82}Se value. Although the ^{214}Bi electron energies were used as a model to compute the contaminant opening angle distribution, the energy dependence is weak, and the mean opening angle computed is valid for other contaminants as well.

G. Additional experimental runs

After the data of Table III had been recorded, changes were made in the apparatus to improve contrast in the photographs. New materials introduced in the chamber increased the radon level by a factor of 10 and reduced the trigger efficiency by a factor of 2.5.

It was found to be possible, by a continuous change of gas in the chamber, to reduce the radon to a level below the original amount, but the maintenance of good cloud chamber performance over extended periods was difficult with the continuous gas flow.

Though data taken under these conditions[10] were not at variance with the older results, it was decided to terminate the experiment and build a new apparatus (see Sec. IV).

H. Overall detection efficiency and the ^{82}Se half-life

The detection efficiency could not be measured directly because no copious source of negatron pairs with the ^{82}Se energy spectrum was available. Two independent methods of efficiency determination were attempted. First, the Monte Carlo calculation described in Sec. III E, gave an overall efficiency $\epsilon = 0.025$. This small number is the product of probabilities for exceeding the energy thresholds (0.30 after ionization losses), for both particles going upward (0.20), for striking the appropriate configuration of proportional counter wires (0.52), showing sufficient track curvature and missing the cloud chamber wall (0.79). Because of assumptions and approximations attending this calculation, the result can be regarded only as an estimate, perhaps valid within a factor of 2.

A second method utilized the negatron pairs from ^{214}Bi, that is, $2e^- + \alpha$ events. The ratio of the number of these pairs observed to the number actually occurring can be used to approximate the detection efficiency for pairs from double beta decay. The numbers of $2e^- + \alpha$ and $e^- + \alpha$ events occurring are related by the internal conversion coefficients in the ^{214}Bi decay scheme. The $e^- + \alpha$ events occurring are, in turn, related to the number observed by the probability of a trigger from a single electron. By this indirect method the number of $2e^- + \alpha$ events occurring, and hence the efficiency, can be calculated as $\epsilon = 0.022$.[10] This value of ϵ is good to perhaps ±30%, with some of the uncertainty arising from the difference between the ^{82}Se double beta decay characteristics and those of the ^{214}Bi beta internal-conversion events used in the derivation. Aside from the bismuth conversion lines, the general distributions of the ^{82}Se and ^{214}Bi energy spectra are quite similar, however (Figs. 17 and 18). The overall detection efficiency is taken to be 0.022 ± 0.007.

A half-life for ^{82}Se can be calculated from this efficiency and from the assumption that the twenty $2e^-$ events observed during the first 37.0 live days were caused only by ^{82}Se and ^{214}Bi. The ^{214}Bi contribution was calculated as 4.8 ± 1.2 in Sec. III B 2. The ^{82}Se portion becomes $(20 \pm 4) - (4.8 \pm 1.2) = 15.2$

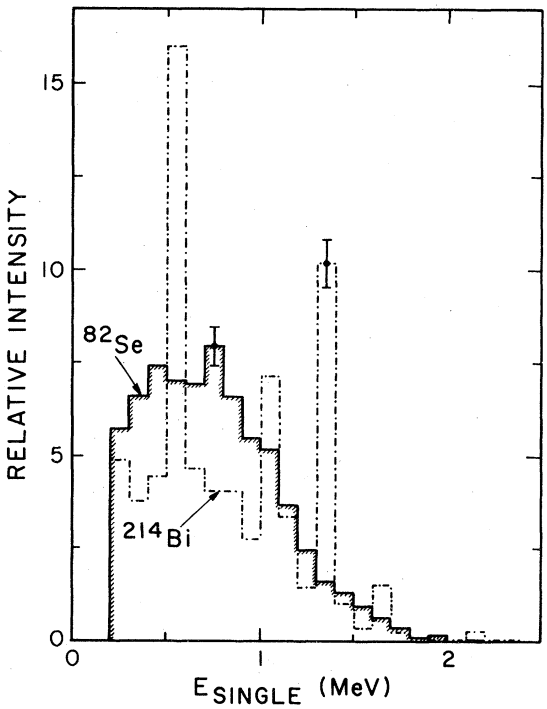

FIG. 17. Monte Carlo generated single electron spectra for negatron pairs from ^{82}Se double beta decay, and from ^{214}Bi beta decay with internal conversion. Note the conversion lines in the ^{214}Bi spectrum. Spectra include the bias of the apparatus.

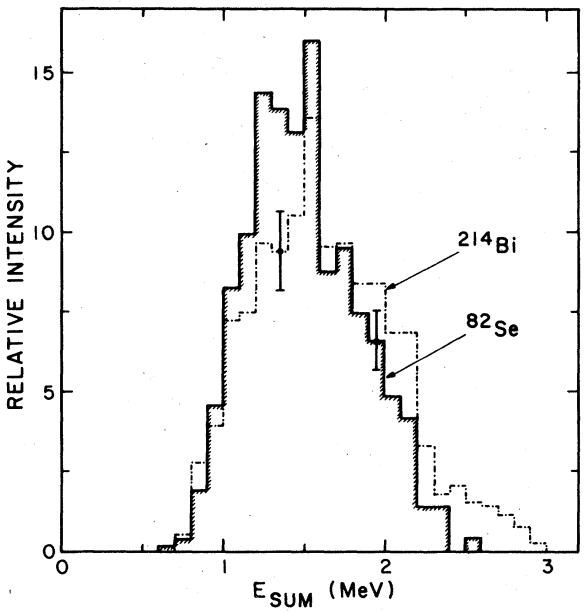

FIG. 18. Monte Carlo generated electron sum spectra for negatron pairs from ^{82}Se double beta decay, and from ^{214}Bi beta decay with internal conversion. Spectra include the bias of the apparatus.

± 4.6. The resulting half-life[10] is

$$T_{1/2} = 1.0 \pm 0.4 \times 10^{19} \text{ yr}.$$

No event was recorded with a sum energy near the 3.0 MeV value corresponding to neutrinoless double beta decay. The experiment was not efficient for neutrinoless detection because of the relatively low source mass, trigger efficiency, and live time. The more energetic neutrinoless events would not be lost to the 1 MeV sum energy threshold, but more would strike the chamber walls or show insufficient track curvature for charge sign determination. Some sensitivity would also be lost to the nominal 3.0 MeV upper bound on the trigger energy window. These factors lead to an estimate of 4% for the overall efficiency for neutrinoless decay. Zero counts at 4% efficiency would result in a 68% confidence limit on the neutrinoless half-life of $>2.4 \times 10^{20}$ yr. The more sensitive neutrinoless measurement of Cleveland, *et al.*[5] resulted in a limit of 3.1×10^{21} yr at the same confidence level.

I. Use of a dummy source

No use was made of a normal isotopic selenium dummy source in this experiment. Because troublesome levels of contamination can be below the sensitivity of low-background counting facilites, it is possible for a double beta decay source to harbor more clandestine radioactivity than its dummy counterpart. Consequently, the absence of negatron pairs from a dummy is not a sufficient condition to assign to double beta decay the negatron pairs from the genuine material. Nor is it a necessary condition, for the contamination levels could be reversed. Rather than use a dummy source to distinguish double beta decay, the present work attempted to recognize false events, and to focus on the distinctive character of the opening angle distribution and ^{82}Se energy spectra.

IV. A FOLLOW-UP EXPERIMENT USING A TPC

A new apparatus has been designed with the intention of increasing the sensitivity to double beta decay, both with and without neutrinos. The system will operate as a time projection chamber (TPC) with tracks of ionization electrons drifting into end planes of individually read proportional wires, much as in the TPC being constructed for the positron electron project (PEP) facility at SLAC.[16] The ^{82}Se source will form the central negative high voltage plane. Electrons from ionization of helium gas will drift perpendicularly away from the source and parallel to a magnetic field.

The demands on this equipment are greatly relaxed compared with those placed on the PEP device. Cost and complexity are correspondingly very much less. The concept is well suited to double beta decay detection, inasmuch as the ability to recognize delayed alpha particles is preserved, while the cloud chamber's long dead time, low efficiency, and disturbance by continuous gas flow are avoided.

This device is now under construction. The anticipated order-of-magnitude improvement in the detection rate for two-neutrino double beta decay should reveal very quickly whether the surprisingly short ^{82}Se half-life apparent in the cloud chamber is, in fact, correct. After about 4 months of running, the new apparatus should also begin to test the neutrinoless limit.

V. CONCLUSIONS

The combination of a thin source and a long period of post-trigger sensitivity has revealed delayed alpha particles attending nearly half of the negatron pairs observed in this search for double beta decay of ^{82}Se. The alpha particle "flag" has transformed an otherwise serious ^{214}Bi background into a useful calibrator of energy spectra, opening angle distributions, and detector efficiency.

Internal conversion has been identified as the predominant mechanism for background production. This understanding made possible the calculation of energy spectra and opening angle distributions of negatron pairs from suspected contam-

inants, and served to reveal differences between those pairs and the alpha-unaccompanied negatron pairs actually observed.

With the exception of a small residual background from decay of ^{214}Bi, where the delayed alpha particle is trapped within the source, the common radionuclides of the uranium series, thorium series, and other ubiquitous sources do not seem to be contributing. The 20 observed unaccompanied negatron pairs are distributed in energy and opening angle in a manner consistent with ^{82}Se double beta decay with neutrinos. The evidence is statistically fragile, however, and is regarded as suggestive but not conclusive evidence for double beta decay.

The value $1.0 \pm 0.4 \times 10^{19}$ yr implied by this experiment for the ^{82}Se half-life is more than an order of magnitude smaller than numbers reported for geochemical measurements (e.g., 2.76×10^{20} yr, Srinivasan *et al.*[2]). The disparity could be explained if the product krypton diffused out of the salenium ore over geologic time. However, geochemical evidence does not support diffusion of this magnitude for the heavier noble gases. The disagreement is serious, and one should be wary of accepting a shorter half-life before a definitive direct counting experiment is performed.

Some of the early theoretical calculations of the ^{82}Se half-life were uncertain by several orders of magnitude, and allowed both the present result and the geochemical number within the error. Recently, matrix elements for ^{82}Se double beta decay have been calculated by Haxton and Stephenson,[17] who report much tighter error limits. Their half-life is consistent with the present experiment, and clearly disagrees with the geochemical value.

The streamer chamber experiment leading to the neutrinoless $\beta\beta$ limit reported by Cleveland *et al.*,[5] also yielded data that could be interpreted in terms of two-neutrino decay. If the majority of negatron pairs from the selenium source in that experiment are assigned to double beta decay, the resulting two-neutrino half-life agrees with $1.0 \pm 0.4 \times 10^{19}$ yr value of the present work. The collaborators on the Cleveland experiment feel that such an assignment is unjustified, however, because of disagreement with a $1-\cos\theta$ opening angle distribution, and because a normal isotopic selenium dummy source gave a similar rate of activity. They declined to subtract the dummy source rate as background because the ^{82}Se and dummy sources were not necessarily identically contaminated. Instead, in an unpublished analysis, they assigned to double beta decay only those ^{82}Se source events having opening angles greater than 100°, with a corresponding reduction in overall efficiency. The resulting two-neutrino half-life limit is $\gtrsim 3 \times 10^{19}$ yr at a 68% confidence level.[18] The requirement for a definitive experiment again is apparent.

If the half-life is indeed 1.0×10^{19} yr, the ratio

$$R(^{82}\mathrm{Se}) = \frac{\text{neutrinoless rate}}{\text{total rate}} \cong \frac{T_{1/2}(2\nu)}{T_{1/2}(0\nu)} \lesssim \frac{1.0 \times 10^{19}\ \text{yr}}{3.1 \times 10^{21}\ \text{yr}} = 0.003\,,$$

where the direct-counting lower limit of Cleveland *et al.* was used for $T_{1/2}(0\nu)$. This value of $R(^{82}\mathrm{Se})$ is well below the 3–9% range for lepton-nonconserving decay hinted at by Bryman and Picciotto.[1] The upper limit on the lepton-nonconserving fraction of the weak interaction amplitude reported by Cleveland *et al.* is multiplied by $\sim(1.0 \times 10^{19}/2.76 \times 10^{20})^{1/2}$, reducing it from $\sim 3 \times 10^{-4}$ to $\sim 6 \times 10^{-5}$.

The time projection chamber now being constructed is intended to probe with greater sensitivity the reduced upper limit on lepton number violation implied by the cloud chamber experiment.

ACKNOWLEDGMENTS

We express our gratitude to Frederick Reines whose longtime interest in double beta decay nurtured this effort from its inception. He arranged the procurement of the cloud chamber and called our attention to the availability of the enriched ^{82}Se. He provided challenging discussions throughout the course of the experiment. We thank Arnold F. Clark and E. W. Cowan who graciously offered assistance in our struggle with the idiosyncrasies of the Wilson cloud chamber. We gratefully acknowledge helpful suggestions by H. H. Chen, J. F. Lathrop, R. D. Newman, and A. M. Rushton, and the technical assitance of August Hruschka and Herb Juds. This work was supported by the U. S. Department of Energy.

---

*Present address: Mathematical Sciences North West, Inc., Bellevue, Washington.

[1] D. Bryman and C. Picciotto, Rev. Mod. Phys. 50, 11 (1978).

[2] B. Srinivasan, E. C. Alexander, Jr., R. D. Beaty, D. E. Sinclair, and O. K. Manuel, Econ. Geol. 68, 252 (1973).

[3] T. Kirsten and H. W. Müller, Earth Planet. Sci. Lett. 6, 271 (1969). A subsequent, more detailed analysis can be found in the unpublished dissertation by H. W. Müller, Ruprecht-Karl-Universität, Heidelberg (1971). Here a linear relationship is shown between the ^{82}Kr/Se ratio and the age of the selenium ore, for six ore samples spanning more than 2×10^9 yr. Five of the samples are assigned ages clustering between (0.8 and 2.9) $\times 10^8$ yr. The 2.4×10^9 yr age of the sixth was deter-

mined by ^{130}Te-^{130}Xe dating based on a geochemical ^{130}Te $\beta\beta$-decay half-life. Disagreement of K-Ar and geologic ages in some samples is attributed to stray radiogenic argon.

[4]E. W. Hennecke, O. K. Manuel, and D. D. Sabu, Phys. Rev. C 11, 1378 (1975).

[5]B. T. Cleveland, W. R. Leo, C. S. Wu, L. R. Kasaday, A. M. Rushton, P. J. Gollon, and J. D. Ullman, Phys. Rev. Lett. 35, 757 (1975).

[6]A preliminary report of the present work was published in *Proceedings of the International Neutrino Conference, Aachen, West Germany, 1976*, edited by H. Faissner, H. Reithler, and P. Ferwas (Vieweg, Braunschweig, West Germany, 1977).

[7]R. K. Bardin, P. J. Gollon, J. D. Ullman, and C. S. Wu, Nucl. Phys. A158, 337 (1970).

[8]R. Bailey (private communication).

[9]J. A. Bruner, Phys. Rev. 84, 282 (1951).

[10]A more detailed discussion can be found in University of California, Irvine, Report No. UCI-10P19-143, 1979 (unpublished).

[11]A. F. Clark *et al.*, Phys. Rev. Lett. 27, 51 (1971).

[12]D. D. Lowenthal, Doctoral thesis, University of California, Irvine, 1976 (unpublished).

[13]P. J. Soilleux, Health Phys. 18, 245 (1970).

[14]C. M. Lederer and V. S. Shirley, *Tables of Isotopes*, 7th ed. (Wiley, New York, 1978).

[15]S. Bjørnholm and O. B. Nielsen, Nucl. Phys. 42, 642 (1963).

[16]A. R. Clark *et al.*, Proposal for a PEP Facility based on the Time Projection Chamber, PEP 4, 1976.

[17]W. C. Haxton and G. J. Stephenson (private communication).

[18]B. T. Cleveland and J. D. Ullman (private communication).

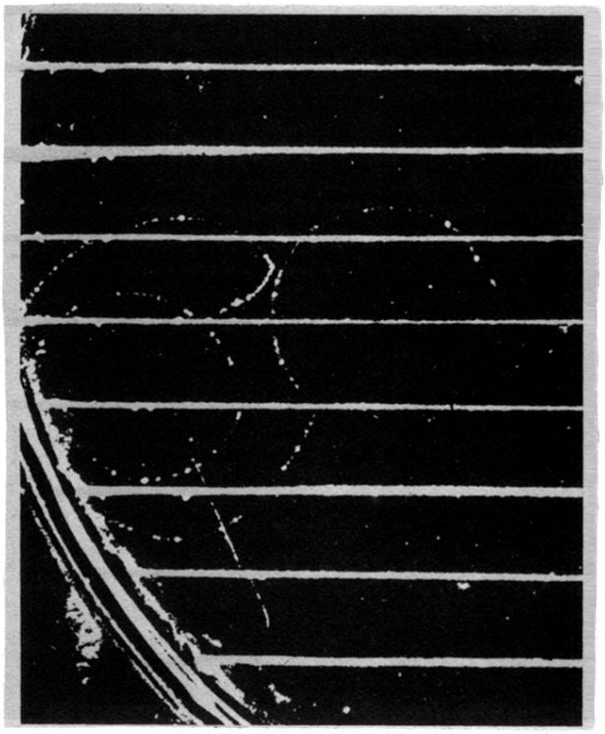

FIG. 3. A cloud chamber photograph of a negatron pair ($2e^-$) originating from one of the ^{82}Se source strips. The electrons pass through the strips quite freely.

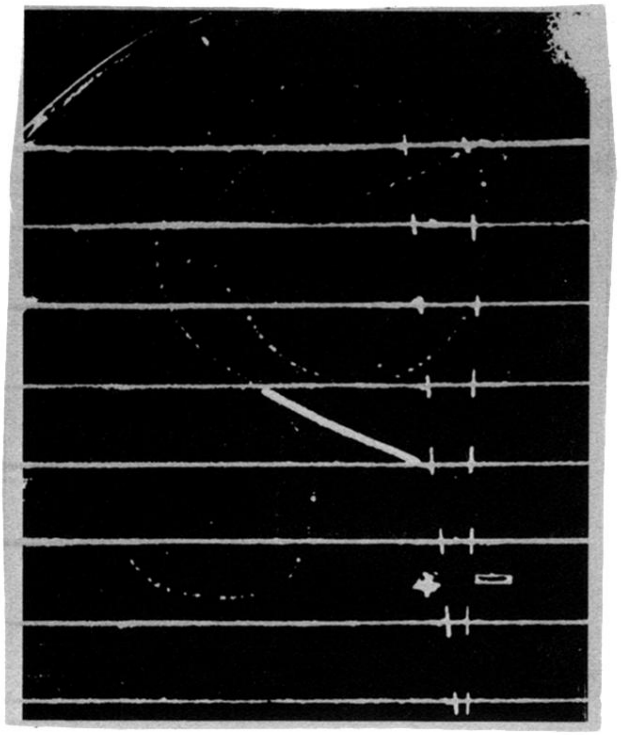

FIG. 4. A negatron pair from bismuth contamination as revealed by an accompanying alpha particle ($2e^{-} + \alpha$).